A Quantitative Study of the Synthesis of TiB_2 Particles *via* Salts-Metal Reaction at Different Temperatures

ZHIWEI LIU, QINGYOU HAN, ZHIFU HUANG, and JIANDONG XING

This research quantitatively studied the effect of temperature on the synthesis of TiB_2 particle reinforcement *via* a casing method in which a salts-metal reaction was involved. Experimental results showed that the yield of TiB_2 reached 89.5 pct and most TiB_2 particles ranged from 400 to 800 nm at 1173 K (900 °C) with a 10-minute reaction time; when the reaction time was 30 minutes, the TiB_2 particles had similar yield and size distribution. At 973 K (700 °C) with a 10-minute reaction time, most TiB_2 particles were less than 300 nm, whereas the yield was just 28.1 pct; as the time was prolonged to 30 minutes, some smaller-sized TiB_2 particles were synthesized and the yield of TiB_2 was 36.4 pct. At a higher temperature [1173 K (900 °C)], the synthesis of TiB_2 mainly followed the precipitation-growth process at reaction interface. At a lower temperature [973 K (700 °C)], the precipitation-growth process and dissolution reaction between Al_3Ti and AlB_2 both contributed to the formation of TiB_2.

DOI: 10.1007/s11661-015-3268-7

I. INTRODUCTION

IT is well known that *in situ* TiB_2 particles can be synthesized *via* the salts-metal reaction by adding the mixed K_2TiF_6-KBF_4 salts into molten Al at high temperatures.[1,2] Due to its unique characteristics, such as low cost, high efficiency and short synthesizing time, the salts-metal reaction has been widely used in practical productions for producing *in situ* TiB_2/Al composites and the existence of TiB_2 particles can improve the mechanical properties of the Al alloys significantly.[3,4] This type of material has been obtained more attentions in the aerospace and automobile industries. In nature, the salts-metal reaction belongs to a chemical reaction. The synthesizing temperature is one of the most important factors, which influences the formation of the products during the reaction. Generally, a high temperature is beneficial for the formation of TiB_2 particles, and the temperature used in the salts-metal reaction is usually higher than 1073 K (800 °C). It has been reported that a lower temperature can lead to the formation of Al_3Ti and AlB_2 phases, which decrease the yield of TiB_2 phase in the Al matrix.[5] Thereby, using a higher temperature of the Al melt is always recommended in order to improve the production of TiB_2 particles in the reaction.

Although the salts-metal reaction has become the most common method for synthesizing *in situ* TiB_2/Al composites, the relationship between the temperature and the formation of TiB_2, however, has not been investigated clearly. A quantitative study of the effect of temperature on the synthesis of TiB_2 regarding the yield of TiB_2 particles and their size distribution has not been reported by other researchers. In addition, the understanding of the formation mechanism of TiB_2 in the salts-metal reaction is still unclear.

So far, two main viewpoints with regard to the formation process of TiB_2 have been proposed. One refers that TiB_2 particles are formed by a dissolution-precipitation mechanism when the concentrations of Ti and B reach saturation in molten Al (alloys).[6] The detailed mechanism can be summarized as follows.

First, K_2TiF_6 and KBF_4 are melted on the Al surface, both of which are separately decomposed to KF (liquid), TiF_4 (gas), and BF_3 (gas), which are expressed as follows:

$$K_2TiF_6(l) \rightarrow 2KF(l) + TiF_4(g) \quad [1]$$

$$KBF_4(l) \rightarrow KF(l) + BF_3(g). \quad [2]$$

Then, Ti and B atoms are released and diffuse into liquid Al through the aluminothermic reduction of TiF_4 and BF_3 gases at the salts-melt interface, which are expressed as below:

$$TiF_4(g) + [Al] \rightarrow [Ti]_{Al} + AlF_3(l) \quad [3]$$

ZHIWEI LIU, Associate Professor, is with the State Key Laboratory for Mechanical Behavior of Materials, School of Materials Science and Engineering, Xi'an Jiaotong University, Xi'an 710047, P.R. China, and also with the School of Engineering Technology, Purdue University, 401 North Grant Street, West Lafayette, IN 47906. Contact e-mails: liuzhiwei@mail.xjtu.edu.cn; lzw_6260@163.com QINGYOU HAN, Professor, is with the School of Engineering Technology, Purdue University. Contact e-mail: hanq@purdue.edu ZHIFU HUANG, Associate Professor, and JIANDONG XING, Professor, are with the State Key Laboratory for Mechanical Behavior of Materials, School of Materials Science and Engineering, Xi'an Jiaotong University.

Manuscript submitted February 21, 2015.
Article published online December 10, 2015

$$BF_3(g) + [Al] \rightarrow [B]_{Al} + AlF_3(l). \quad [4]$$

When the solutes [Ti] and [B] in liquid Al reach saturation, they might be separated out as compounds Al_3Ti, AlB_2, and TiB_2, according to the following reactions:

$$[Ti]_{Al} + 3[Al] \rightarrow Al_3Ti \quad [5]$$

$$2[B]_{Al} + [Al] \rightarrow AlB_2 \quad [6]$$

$$[Ti]_{Al} + 2[B]_{Al} \rightarrow TiB_2. \quad [7]$$

Among the compounds involved in the salts-metal reaction, TiB_2 is the most thermodynamically stable phase due to its lowest free energy of formation.[7] The overall reaction showing the formation of TiB_2 can be written as

$$3K_2TiF_6 + 6KBF_4 + 10Al \rightarrow 3TiB_2 + 12KF + 10AlF_3. \quad [8]$$

The other one refers that TiB_2 particles are synthesized resulting from the reaction between Al_3Ti and AlB_2, which are formed due to the reactions of K_2TiF_6-Al and KBF_4-Al.[8] The following reactions describe the formation process of TiB_2:

$$3K_2TiF_6 + 13Al \rightarrow 3Al_3Ti + 3KAlF_4 + K_3AlF_6 \quad [9]$$

$$2KBF_4 + 3Al \rightarrow AlB_2 + 2KAlF_4 \quad [10]$$

$$Al_3Ti + AlB_2 \rightarrow TiB_2 + 4Al. \quad [11]$$

An overall reaction for synthesizing TiB_2 can be given as follows:

$$3K_2TiF_6 + 6KBF_4 + 10Al \rightarrow 3TiB_2 + 9KAlF_4 + K_3AlF_6. \quad [12]$$

Actually, the above two mechanisms are based on the equilibrium thermodynamics of the Al-Ti-B system. The practical salts-metal reaction, however, is a typical non-equilibrium thermodynamic reaction. An analysis considering the reaction temperature and reaction time might be more suitable to reflect the actual formation process of TiB_2 during the reaction.

In order to investigate the influences of reaction temperature and time on the formation of TiB_2 particles in molten Al regarding the yields and size distributions of TiB_2 particulates, two reaction temperatures [1173 K and 973 K (900 °C and 700 °C)] with two reaction times (10 and 30 minutes) were studied. A quantitative analysis about the formation of TiB_2 under different experimental parameters was firstly investigated in this research. The formation process of TiB_2 particles was also explored from the perspective of the temperature.

II. EXPERIMENTAL

A. *Synthesis of TiB_2 Particles via Salts-Metal Reaction*

A 500 g pure Al ingot was melted in a graphite crucible in an electrical resistant furnace. After the temperature of the Al melt reached and kept stable at 1173 K (900 °C) [or 973 K (700 °C)], the mixed K_2TiF_6-KBF_4 salt powders were added into the Al melt, and the addition of the mixed salts corresponded to the composition of Al-5 wt pct TiB_2. Then the melt was stirred manually for a few seconds by using a niobium bar. After 10 min, the Al melt containing reaction products was stirred again, for the newly formed products might deposit during the reaction due to the higher density than pure Al. After the slag on the melt surface was removed, the melt was poured into a steel mold to form an ingot. For the samples fabricated in 30 min, the melt was stirred in 10-minute intervals. 4 samples were fabricated in total. For simplicity, the 4 samples were referred as S900-10, S900-30, S700-10, and S700-30, respectively (the first and second numbers stands for the reaction temperature (°C) and time (minutes) in each sample).

B. *Extraction Procedure for Obtaining TiB_2 Particles*

In this research, some TiB_2 particles were extracted from each sample for calculating the yield of TiB_2 particles and measuring their size distribution. The detailed extraction procedure for obtaining TiB_2 particles is given as (1) A small ingot was cut from the sample, and the surface of which was cleaned by sand paper. (2) The small ingot was dissolved in a 15 vol pct aqueous HCl solution in a beaker at room temperature. After dissolution, a layer of particles were deposited at the bottom of the beaker, and then the HCl solution was decanted. (3) TiB_2 particles were washed with water for several times until the supernatant displayed neutral pH. (4) These TiB_2 particles were washed with ethanol, and then dried by using an electric hair dryer. According to our proceeding work,[9] pure TiB_2 phase can be obtained through the above process and no other phases can influence the calculation of the yield of TiB_2 particles and the measurement of their size distribution.

C. *Examination of Samples*

In each group of experiment, the products generated in the reaction were consisted of ingot and slag. A small sample was cut from the ingot, and ground using SiC sand papers successively following the order of 180, 240, 400, and 600 mesh. Then the ground sample was polished using micro-sized diamond compound, following the order of 3 and 1 μm. After that the polished sample was cleaned in the ultrasonic cleaner for a few minutes to clean the polished surface. The by-product slag was milled to powders by using a glass mortar.

The sample and slag powder were both examined by X-ray diffraction (XRD, Bruker D8, AXS, Karlsruhe, Germany) using Cu Kα radiation at 40 kV and 40 mA and a scan rate of 0.10°/s. The microstructures of

samples were analyzed by scanning electron microscopy (SEM, S-4800, Hitachi, Ltd., Tokyo, Japan) equipped with an energy dispersive spectroscope (EDS) device for identifying the components in the samples. An optical microscopy (OM) was also applied to observe the microstructures of samples.

D. *Calculation of the Yield of TiB_2 Particles*

Three small ingots with a weight of about 8 grams cut from each sample were treated by a completed extraction process, respectively. Three groups of extracted powders were weighted by using an electric balance. Then the actual weight percentage of TiB_2 phase in the Al matrix could be calculated. Since the sample was fabricated corresponding to the composition of Al-5 wt pct TiB_2, the yield of TiB_2 could be further obtained. An average value of the yield was computed in order to decrease the experimental error.

E. *Measurement of the Size Distributions of TiB_2 Particles*

Zetasizer Nano ZS (Malvern) was used to measure the size distributions of TiB_2 particulates extracted from each sample. This device was able to measure the particles with the size ranging from 3 nm to 5 μm. Before the test, a small amount of TiB_2 powders were diluted with DI water. In order to reduce error, 10 measurements were conducted for each sample.

III. RESULTS AND DISCUSSION

A. *S900-10 Sample*

1. *XRD analysis*

Figure 1 shows the XRD patterns of the slag and sample produced at 1173 K (900 °C) with a 10-minute reaction time. It is obvious that $KAlF_4$ and K_3AlF_6 were the two main phases in the slag, as shown in Figure 1(a), indicating that Ti and B elements were both transferred from the molten mixed salts to molten Al. In the S900-10 sample, TiB_2 was the only newly formed phase during the salts-metal reaction, the diffraction peaks of which could be observed clearly, as shown in Figure 1(b) (inset graph). The results of the two XRD patterns indicate that the chemical formula shown in reaction [12] is more suitable to describe the process of the reaction of K_2TiF_6-KBF_4-Al system.

2. *SEM analysis*

Figure 2 shows the typical microstructure of the S900-10 sample. Only one type of newly formed phase existed in the Al matrix, which was identified as TiB_2 by EDS. These small-sized TiB_2 particulates aggregated to form clusters at α-Al grain boundaries, as shown in Figure 2(a). Figure 2(b) clearly shows that these TiB_2 particles synthesized *via* the salts-metal reaction had different sizes, and most of them were much smaller than 1 μm. In Figure 2(c), it can be found that some TiB_2 particles had a larger size exceeding 1 μm.

B. *S900-30 Sample*

1. *XRD analysis*

Figure 3 shows the XRD patterns of the slag and sample (S900-30) produced at 1173 K (900 °C) with a 30-minute reaction time. Similar to the products produced at 1173 K (900 °C) with a 10-minute reaction time, $KAlF_4$ and K_3AlF_6 were the two main phases in the slag (Figure 3(a)), and TiB_2 was the only newly formed phase in the sample (Figure 3(b)).

2. *SEM analysis*

The typical microstructure of the S900-30 sample is presented in Figure 4. Overall, it had similar microstructural features with the S900-10 sample. Only TiB_2 particulates were *in situ* formed, which existed in the Al matrix as clusters located at the grain boundaries (Figure 4(a)). Most TiB_2 particles were smaller than 1 μm in size (Figure 4(b)), whereas a very small amount of TiB_2 particles were greater than 1 μm, as shown in Figure 4(c).

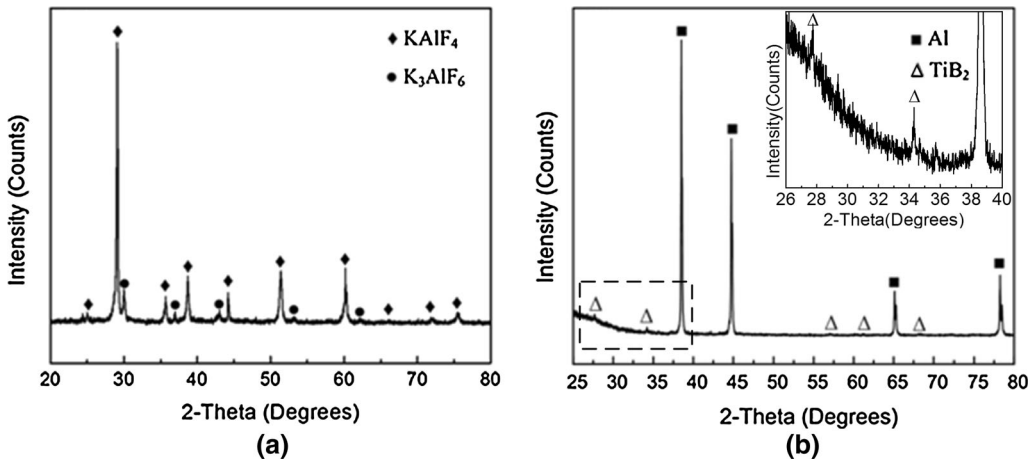

Fig. 1—XRD patterns of the slag (*a*), and S900-10 sample (*b*) produced at 1173 K (900 °C) with a 10-min reaction time.

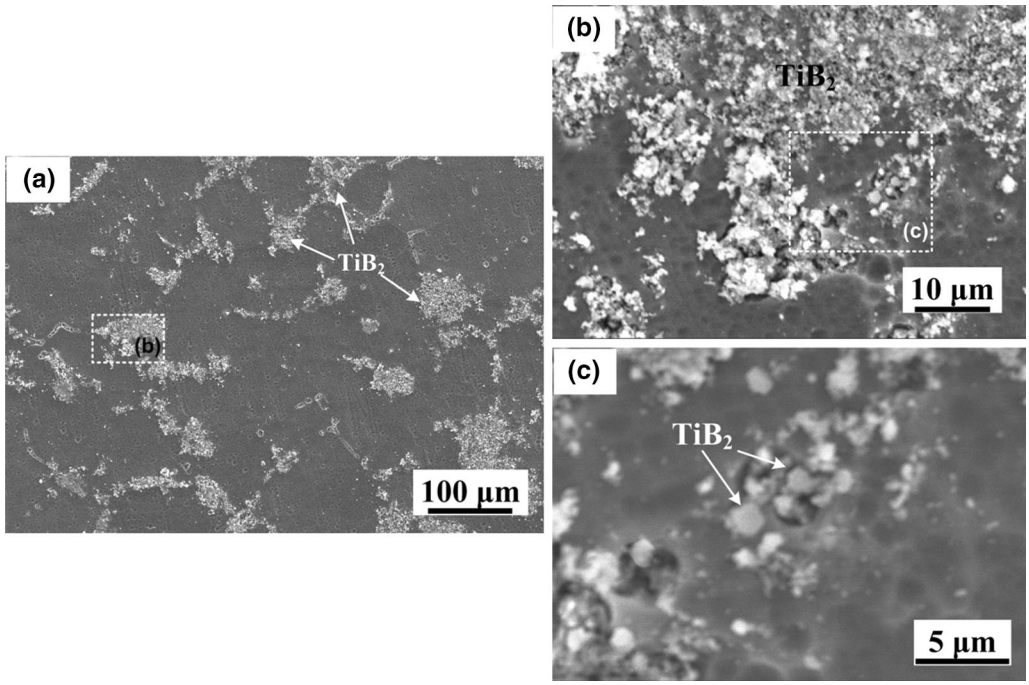

Fig. 2—(*a*) Typical microstructure of the S900-10 sample, (*b*) higher magnification of the area marked in image (a), and (*c*) higher magnification of the area marked in image (b).

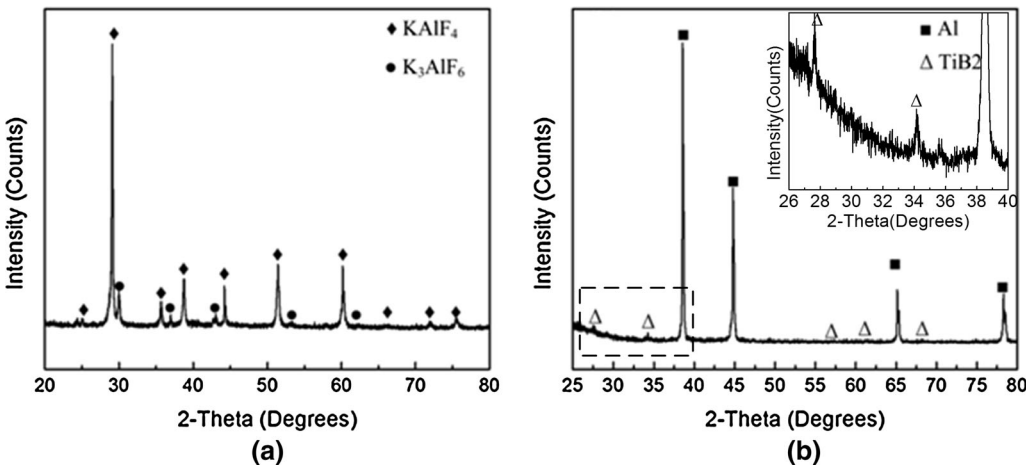

Fig. 3—XRD patterns of the slag (*a*), and S900-30 sample (*b*) produced at 1173 K (900 °C) with a 30-min reaction time.

C. *S700-10 Sample*

1. *XRD analysis*

Figure 5 shows the XRD patterns of the slag and S700-10 obtained in the salts-metal reaction at 973 K (700 °C) with a 10-minute reaction time. $KAlF_4$ and K_3AlF_6 detected by XRD were the main phases in the slag, as shown in Figure 5(a). No phase containing obvious Ti or B was found in the slag, suggesting that Ti and B elements were both transferred to molten Al from salts. Some rather weak diffraction peaks of TiB_2 phase were found in the S700-10 sample (Figure 5(b)), indicating that the mixed-salts reaction proceeded according to the chemical formula shown in reaction [12] at the low temperature of 973 K (700 °C).

2. *SEM analysis*

Figure 6 shows the typical microstructure of the S700-10 sample. Three types of reinforcements existed in the Al matrix. Some blocky particles ranged in size from 1 to 3 μm were detected as Al_3Ti by EDS. Some rather small-sized TiB_2 particles were also found in the matrix, most of which existed along the chain-like reinforcement. After examined by EDS, the main phase of chain-like reinforcement was identified as Al_3Ti, and also some separately tiny TiB_2 particles were located in Al_3Ti, as shown in Figure 6(b). Since the content of Al_3Ti phase in the matrix was rather low, it is hard to detect in the XRD examination (Figure 5(b)). In addition, a little amount of AlB_2 phase might exist in the Al

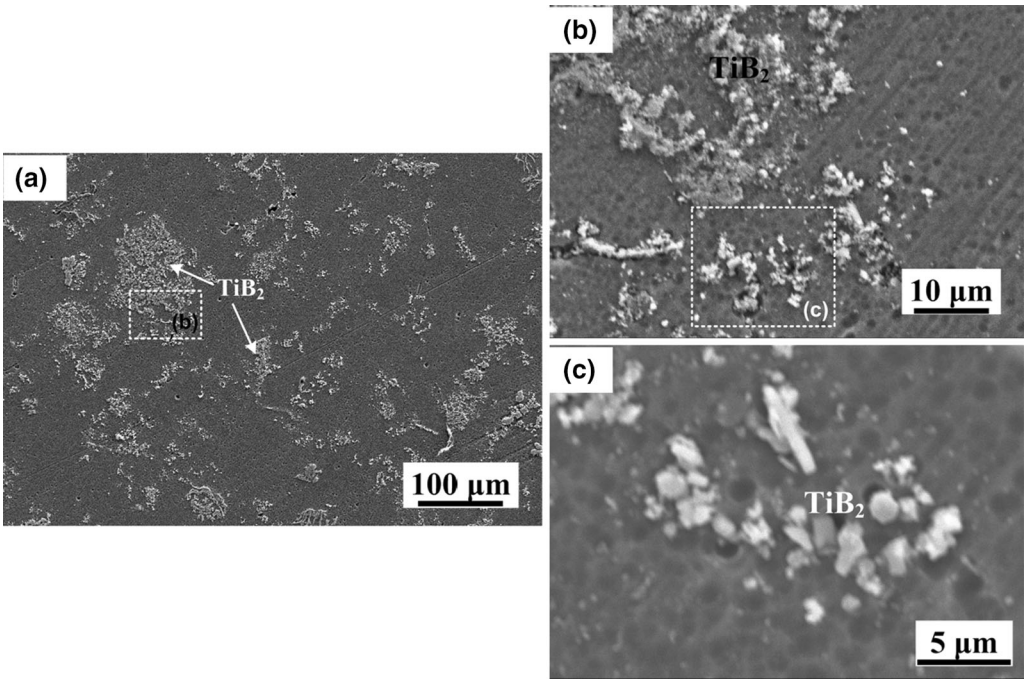

Fig. 4—(*a*) Typical microstructure of the S900-30 sample, (*b*) higher magnification of the area marked in image (a), and (*c*) higher magnification of the area marked in image (b).

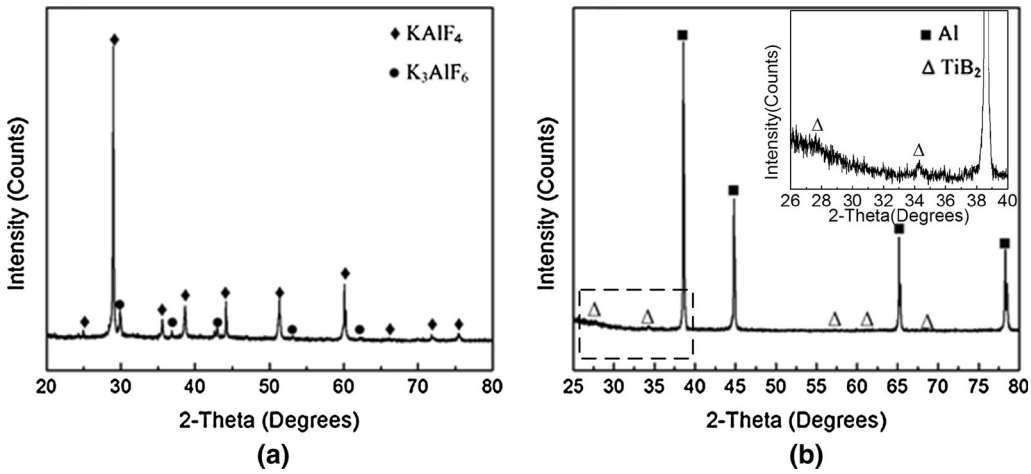

Fig. 5—XRD patterns of the slag (*a*), and S700-10 sample (*b*) produced in the mixed-salts reaction at 973 K (700 °C) with a 10-min reaction time.

matrix, but it is hard to examine them out in the present research due to the limitation of device.

D. *S700-30 Sample*

1. *XRD analysis*

Figure 7 shows the XRD patterns of the slag and S700-30 sample obtained in the salts-metal reaction at 973 K (700 °C) with a 30-minute reaction time. As shown in Figure 7(a), the slag was consisted of $KAlF_4$ and K_3AlF_6 phases. Weak TiB_2 peaks were also found in the sample, showing that the content of TiB_2 phase was still low (Figure 7(b)) in the Al matrix by a 30-minute reaction.

2. *SEM analysis*

Figure 8 shows the microstructure of the S700-30 sample. Long chain-like reinforcements and cluster-like reinforcements were both found in the Al matrix, as shown in Figure 8(a). It is found that the chain-like reinforcement was composed of Al_3Ti and some small-sized TiB_2 particles which were located in the Al_3Ti phase, as shown in Figure 8(b). The cluster-like reinforcement was consisted of some large-sized blocky Al_3Ti particles and some nanometer-sized TiB_2 particles, as shown in Figure 8(c). One more thing should be mentioned is that the size of long chain-like reinforcement in S700-30 sampler was smaller than that in the

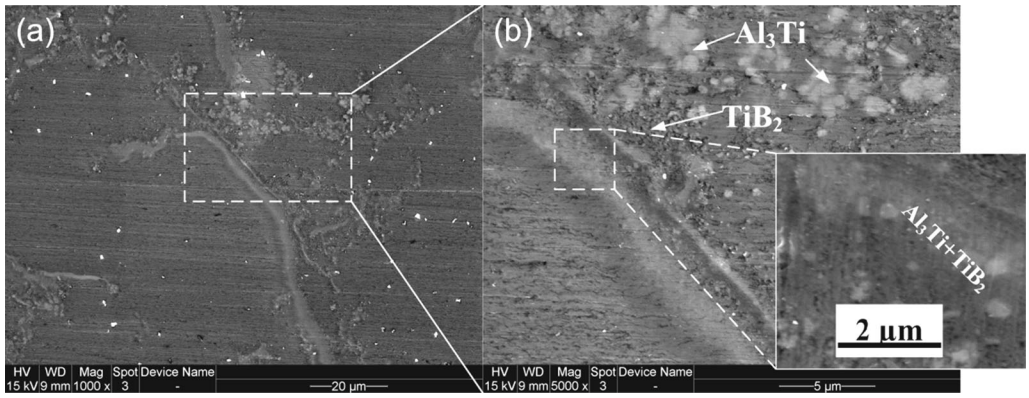

Fig. 6—(*a*) Typical microstructure of the S700-10 sample, and (*b*) higher magnification of the area marked in image (a).

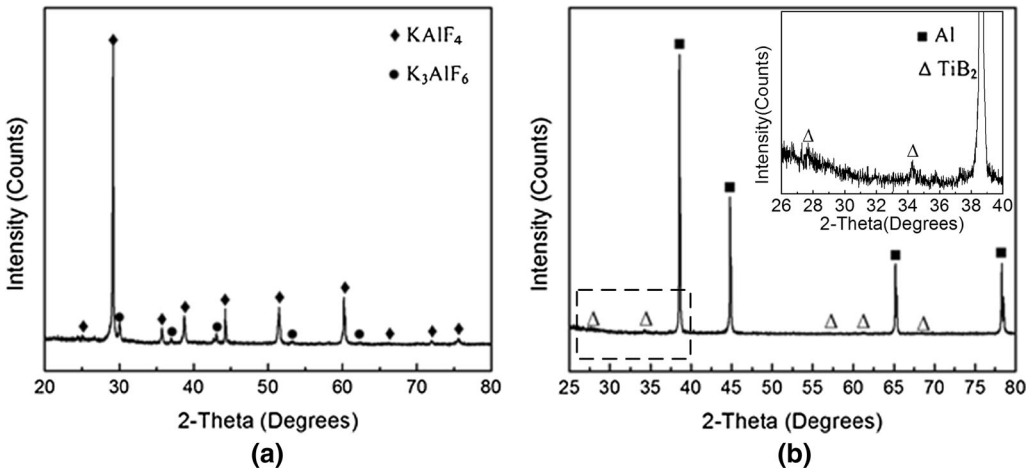

Fig. 7—XRD patterns of the slag (*a*), and S700-30 sample (*b*) produced in the mixed-salts reaction at 973 K (700 °C) with a 30-min reaction time.

S700-10 sample, which indicated that part of it might dissolve or react as the reaction time was increased. AlB_2 phase also might exist in the sample, which was hard to examine out clearly in this research.

E. *Yields and Size Distributions of TiB_2 Particles*

The yields of TiB_2 particles and their size distributions of each sample are presented in Figure 9. For the S900-10 sample, the yields of TiB_2 particles could reach 89.5 pct; most TiB_2 particles were less than 1 μm in size, in which about 81 pct of the TiB_2 particles ranged in size from 400 to 800 nm, and a very small amount of TiB_2 ranged in size from 1 to 2 μm. For the S900-30 sample, the yield of TiB2 particles was about 90.3 pct; overall, the most TiB_2 particles were smaller than 1 μm, in which about 83 pct of the TiB_2 particles ranged in size from 400 to 800 nm, and a rather small amount of TiB_2 particles had the size in the range of 1 to 2 μm. It is clear that the S900-10 and S900-30 samples had similar yield and size distribution of TiB_2 particles. For the S700-10 sample, the yield of TiB_2 particles was rather low, about 28.1 pct; the size of TiB_2 particles was less than 1 μm, in which about 95 pct TiB_2 particles were smaller than 300 nm. For the S700-30 sample, the yield of particles could reach 36.4 pct; more than 95 pct of the TiB_2 had the size less than 300 nm. Comparing with the S700-10 sample, the content of TiB_2 particles with a smaller size was increased in the S700-30 sample, and the ratio of TiB_2 smaller than 100 nm was about 30 pct, indicating a certain amount of TiB_2 particles with a smaller size were formed as the reaction time was prolonged from 10 to 30 minutes.

The results in this research displayed the differences in the formation of TiB_2 at different temperatures [1173 K and 973 K (900 °C and 700 °C)], such as the yields of TiB_2 particulates and their size distributions. It is noted that the reaction temperature played a critical role in the salts-metal reaction of K_2TiF_6-KBF_4-Al system in this research. Accordingly, the related formation mechanism of TiB_2 might be different at different temperatures. The following discussion about the formation process of TiB_2 will be conducted considering the Al melt temperature.

F. *Formation of TiB_2 at a Higher Temperature [1173 K (900 °C)]*

In this research, when the reaction temperature was 1173 K (900 °C) and the reaction time was 10 minutes,

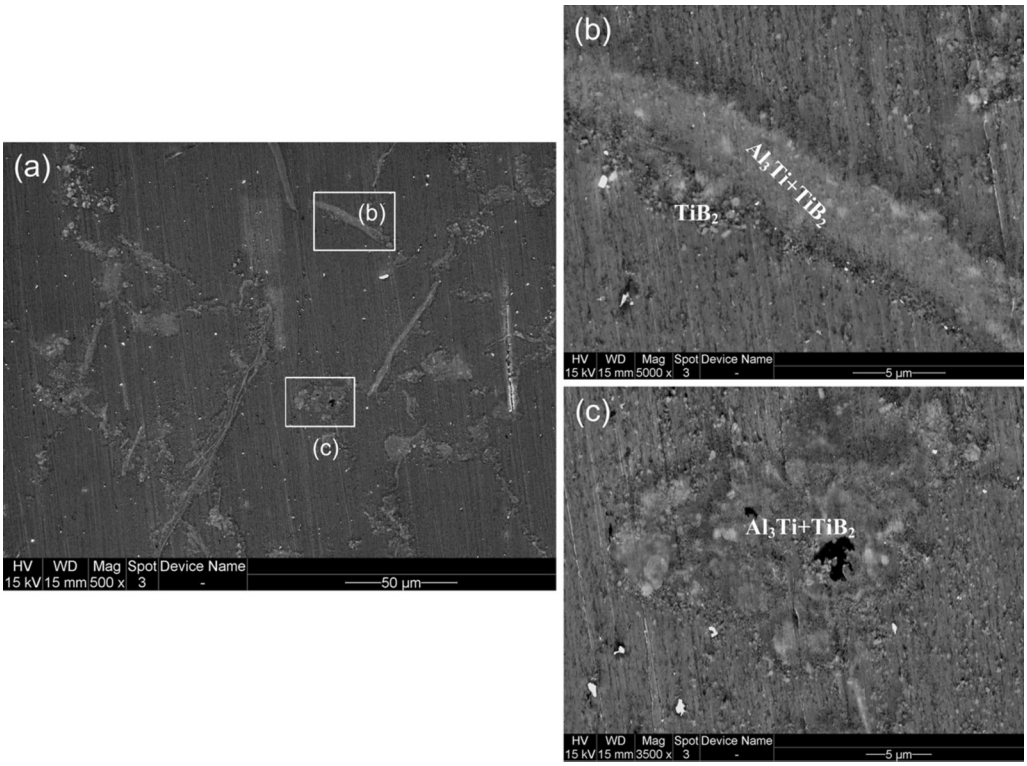

Fig. 8—(*a*) Typical microstructure of the S700-30 sample, and (*b*), (*c*) higher magnification of the areas marked in image (a).

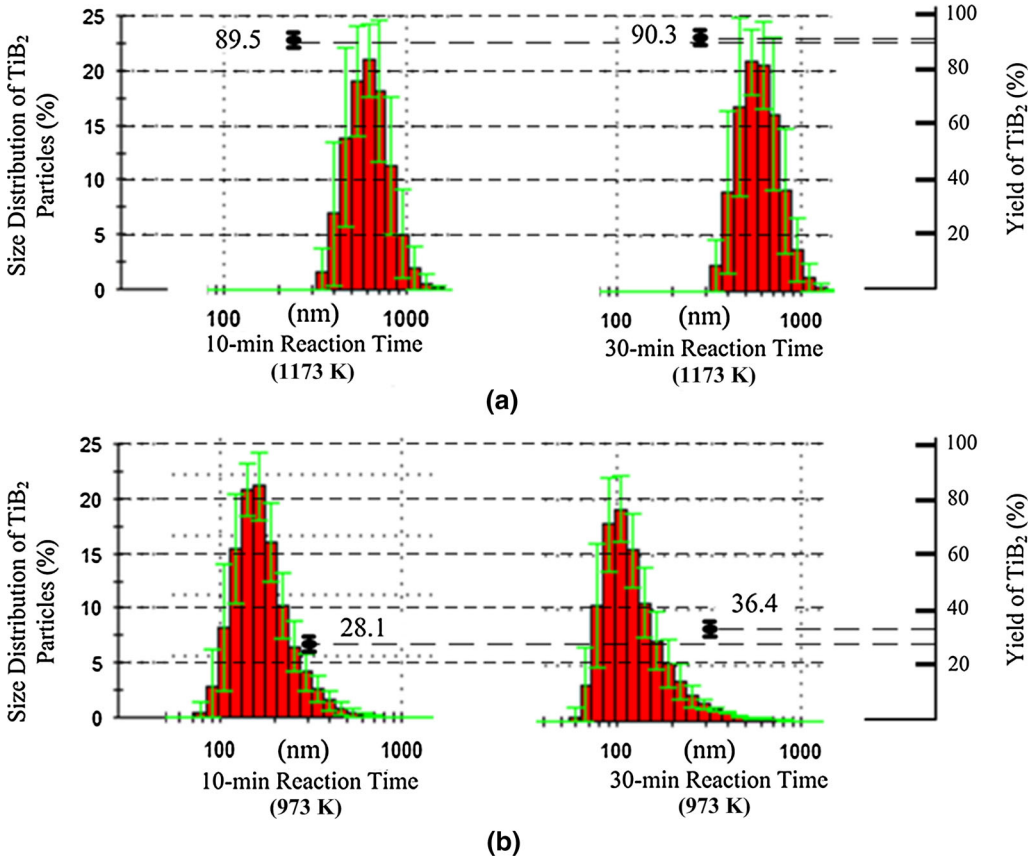

Fig. 9—The yields and size distributions of TiB_2 particles synthesized *via* the salts-metal reactions at 1173 K (900 °C) (*a*) and 973 K (700 °C) (*b*).

no Al_3Ti phase was found in the Al matrix, the yield of TiB_2 reached 89.5 pct, and the size of most of *in situ* formed TiB_2 particulates was in the range of 400 to 800 nm. As the reaction time was increased to 30 minutes, no obvious change occurred in the S900-30 sample, in which the yield of TiB_2 was about 90.3 pct and the size of most TiB_2 particles was in the range of 400 to 800 nm, as shown in Figure 9(a). It is clear that a higher reaction temperature is beneficial for the formation of TiB_2 with a larger size in a short time.

The salts-metal reaction of K_2TiF_6-KBF_4-Al system is an interface reaction. Based on the results of the S900 samples, the possible formation process of TiB_2 phase in the salts-metal reaction is discussed below, in which three critical steps in the reaction are listed, respectively.

1. *Formation of the Interface Between Molten Salts and Al Melt*

First all of, no obvious KF and AlF_3 phases were found in the slags produced in the salts-metal reaction at different temperatures. Thereby, the Ti and B in Al are not from the reactions of TiF_4 (gas)-Al and BF_3 (gas)-Al, in which the TiF_4 and BF_3 gases are from the decomposition of K_2TiF_6 and KBF_4. Accordingly, the formation processes described in reactions [1], [2], [3], and [4] are not suitable to explain the formation of TiB_2 phase. At least, the formation of most TiB_2 phase in the reaction does not follow the chemical reaction shown in reaction [8].

Actually, it has been reported by Birol[10] that even though K_2TiF_6 has a higher melting point than KBF_4, K_2TiF_6 can be reduced by Al, releasing Ti at approximately 493 K (220 °C); KBF_4 starts to be reduced by Al a while later at round 798 K (525 °C), possibly after its polymorphic transformation from orthorhombic to cubic structure is over. In this research, after the mixed salts are added into the molten Al at 1173 K (900 °C), the mixed salts melt quickly on the Al melt surface, and an interface between molten salts and Al melt is formed.

2. *Precipitation of TiB_2*

Once the reaction interface is formed, Ti released from K_2TiF_6 and B released from KBF_4 both react with Al at the interface between salts and Al to form Al_3Ti and AlB_2 by reduction reactions [9] and [10]. According to Al-Ti and Al-B phase diagrams,[11] as shown in Figure 10, Al_3Ti and AlB_2 are both soluble in molten Al. The newly formed Al_3Ti and AlB_2 phases can dissolve in molten Al immediately, and then a thin layer of liquid Al containing Ti and B adjacent to the interface can be formed. The processes can be expressed as follows:

$$AL_3Ti \xrightarrow{\text{dissolving}} [Ti]_{AI} + 3AI \qquad [13]$$

$$AlB_2 \xrightarrow{\text{dissolving}} 2[B]_{Al} + Al \qquad [14]$$

Actually, the above processes are significantly influenced by the temperature of molten Al. Higher contents of [Ti] and [B] in the thin layer are obtained easily at a higher reaction temperature [1173 K (900 °C)]. On the one hand, the reduction reactions between salts and Al become more active, and more Al_3Ti and AlB_2 phases

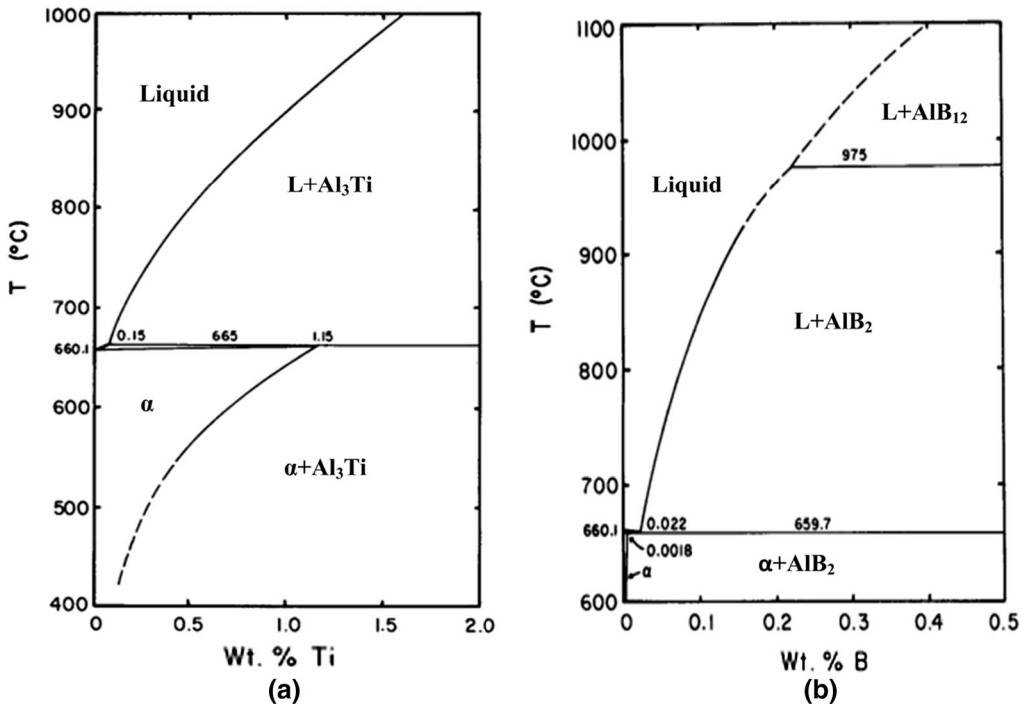

Fig. 10—The aluminum-rich side of the Al-Ti phase diagram (*a*), and the aluminum-rich side of the Al-B phase diagram (*b*). Both of which were reproduced according to Sigworth.[9]

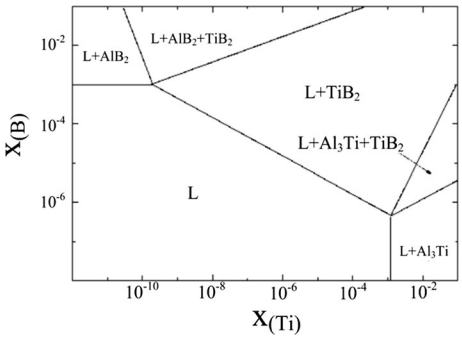

Fig. 11—Phase diagram for Al-Ti-B system at 1000 K (727 °C) (Al corner), x represents the molar fraction, which is reproduced according to Jones and Pearson.[10]

can be obtained at a higher temperature. On the other hand, according to the phase diagrams in Figure 11, the solubilities of Al_3Ti and AlB_2 phases in molten Al become larger as the temperature is increased. Thereby, increasing the temperature can accelerate the transfer speed of Ti and B to molten Al effectively.

As mentioned above, Ti and B can be easily obtained in the thin layer of Al at the reaction interface, and the Ti/B ratio in the reaction layer is much closer to ½ at a higher temperature. When the solutes [Ti] and [B] in liquid Al reaches saturation, they might be separated out as the compounds Al_3Ti, AlB_2, and TiB_2 in the ternary system of Al-Ti-B. TiB_2 is the most thermodynamically stable phase due to its lowest free energy of formation among the three compounds. In addition, according to the phase diagram of Al-Ti-B shown in Figure 11,[12] rather low contents of Ti and B can lead to the formation of TiB_2 phase. In addition, once the concentrations of [Ti] and [B] reach saturation in the Al melt, TiB_2 nuclei precipitate from the saturation region in the Al melt.

3. *Growth of TiB_2*

As the reaction time is increased, more Ti and B are transferred from the molten salts to the reaction layer. TiB_2 particles start to grow up due to the deposition of more Ti and B. It is known that the mass transfers of Ti and B from salts to the reaction interface become faster at a higher temperature, and a higher concentration of solutes in liquid Al can be obtained in a shorter time. Thereby, more Ti and B can be provided in the growth process of TiB_2, and then the TiB_2 particles can grow larger easily. Meanwhile, the salts-melt reaction for synthesizing TiB_2 phase becomes faster.

G. *Formation of TiB_2 at a Lower Temperature [973 K (700 °C)]*

Figure 9(b) shows the yields and size distributions of TiB_2 particulates in the S700 samples. When the salts-metal reaction proceeded at 973 K (700 °C) with a 10-minute reaction time, some Al_3Ti (AlB_2 also should exist) phase existed in the Al matrix, the yield of TiB_2 was just about 28.1 pct, and most of TiB_2 particulates were smaller than 300 nm in size. The yield of TiB_2 fabricated at 973 K (700 °C) with a 30-minute reaction time was 36.4 pct, which was higher than that of TiB_2 in the S700-10 sample by about 29.5 pct. Furthermore, the ratio of TiB_2 particles with a smaller size was increased, which indicated that a certain amount of smaller-sized TiB_2 particles were synthesized as the reaction time was prolonged from 10 to 30 minutes. In addition, according to the SEM analysis (Figures 6 and 8), the products in the S700 samples were more complicated, in which blocky Al_3Ti particulates, tiny TiB_2 particulates, and chain-like Al_3Ti reinforcement containing TiB_2 phase were all formed.

Similarly, a reaction interface between the molten mixed salts and Al is firstly formed in the reaction at a lower temperature. However, more Ti and B might exist as Al_3Ti and AlB_2, respectively, at the reaction interface, because of the limited solubilities of the two phases at a lower temperature (as shown in Figure 10). It has been proved that the reaction between K_2TiF_6 and Al occurs at a much higher rate than that between KBF_4 and Al.[13] Thereby, the ratio of Ti/B in the thinner layer located at the reaction interface is easy to be greater than ½, and this ratio will become greater as the temperature of molten Al is decreased. Part of Ti reacts with B to form TiB_2 phase, following the precipitation-growth process, and the rest of Ti will react with Al to form Al_3Ti phase. As reported by Mohanty *et al.*,[14] the growth of Al_3Ti could engulf the entire TiB_2 particles. Alternatively, the Al_3Ti might also nucleate as individual particulates.[15]

At a lower temperature, since the content of B is rather low in the reaction interface, the growth of TiB_2 will be limited. As a result, the size of TiB_2 in the S700-10 sample was much smaller than that of TiB_2 produced in the S900-10 sample.

In the S700-30 sample, the newly formed TiB_2 particulates had a smaller size. It is reasonable that the newly formed TiB_2 particulates in the S700-30 sample were obtained according to reaction [11], by which Al_3Ti reacted with AlB_2 to form TiB_2. The detailed formation process has been studied by Emamy *et al.*[16] and Michael Rajan *et al.*,[17] respectively. The basic sequence of TiB_2 formation can be proposed as follows:

1. The B from AlB_2 moves toward Al_3Ti phase;
2. Reaction takes place between Ti and B in a gap from Al_3Ti surface to formTiB_2;
3. Dissolution of Al_3Ti phase due to natural cracking and fragmentation of Al_3Ti which lead to increased rate of TiB_2 formation.

These steps involve the dissolutions of AlB_2 and Al_3Ti phases and the reaction for synthesizing TiB_2. Thereby, the related formation process of TiB_2 is a dissolution-reaction process. The detailed process in the present research is give below.

Al_3Ti phase in the S700-10 sample mainly existed in the chain-like reinforcements. The area surrounding Al_3Ti phase was a [Ti]-rich region. AlB_2 phase also existed in molten Al, which could dissolve in Al to generate B atoms. When B atoms contacted with the Al_3Ti phase, Ti and B could react to form TiB_2. The concentrations of [Ti] and [B] were rather low due to the

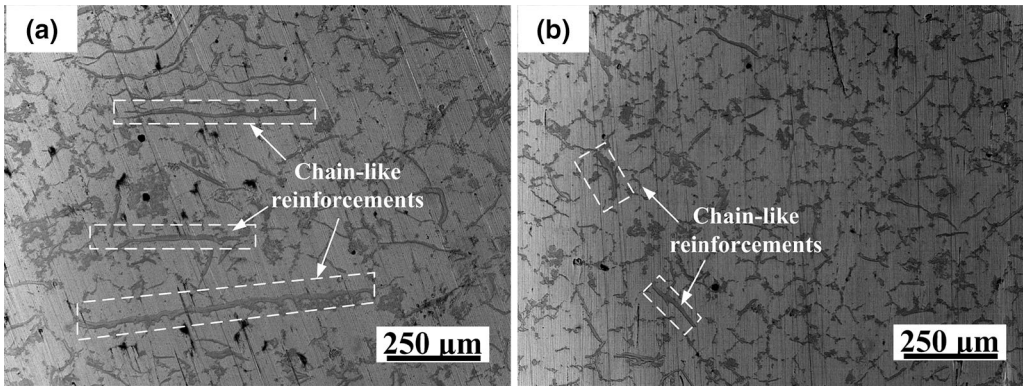

Fig. 12—Microstructures of the S700-10 sample (*a*) and S700-30 sample (*b*).

low temperature of molten Al; thereby, the TiB_2 particles synthesized in this period were not able to grow large, and more TiB_2 particles with a smaller size were formed. As a result, the percentage of TiB_2 particles with smaller size in the S700-30 sample was increased compared with the S700-10 sample, as shown in Figure 9(b).

As the reaction time was increased, the quantities of Al_3Ti and AlB_2 were both decreased, and more TiB_2 could be formed. A comparison about the chain-like reinforcements between the S700-10 sample and the S700-30 sample is given in Figure 12. It is clear that the size of long chain-like reinforcements became small due to the dissolution of Al_3Ti phase in the formation of TiB_2 particulates. In this research, because the temperature was rather low, a complete formation of TiB_2 was hard to achieve in a short holding time. In order to obtain more TiB_2 phase, a longer reaction time is needed. Chen *et al.*[2] reported that a completed reaction for synthesizing TiB_2 could not be achieved with a 60-minute holding time after salt addition at 1023 K (750 °C), and large areas of AlB_2 and Al_3Ti were observed along the grain boundary of the composites. One more thing should be mentioned is about the AlB_2 phase. In this research, the phases in the slags produced in the fabrications of the S700-10 and S700-30 samples were similar; on the other hand, as the content of TiB_2 was increased in the S700-30 sample, it is reasonable to think some AlB_2 should exist in the S700 samples. As reported by Wang *et al.*,[18] blocky AlB_2 could be formed in the Al-B master alloy at 1023 K (750 °C) with a 10-minute reaction time. Wang *et al.*[19] continued proving that the similar AlB_2 particles still existed in the Al-B master alloy at 1023 K (750 °C) with a 30-minute reaction time. Due to the rather small amount of AlB_2, it was hard to be detected by XRD in this research.

IV. CONCLUSIONS

In this research, the influence of reaction temperature on the formation of TiB_2 *via* the salts-metal reaction regarding the yield and size distribution of TiB_2 particles was quantitatively analyzed firstly and the formation processes of TiB_2 at a higher temperature [1173 K (900 °C)] and a lower temperature [973 K (700 °C)] were both investigated as well. The following conclusions are drawn:

1. Reaction temperature has an important influence on the synthesis of TiB_2 in molten Al *via* the salts-metal reaction. A high temperature [1173 K (900 °C)] is beneficial for the formation of TiB_2. A higher temperature can lead to a higher yield of TiB_2 particles with a larger size. In contrast, smaller-sized TiB_2 particles can be obtained at a lower temperature [973 K (700 °C)], but the formation of TiB_2 can be limited significantly, resulting in a rather low yield of TiB_2.
2. At a higher reaction temperature [1173 K (900 °C)], the salts-metal reaction for synthesizing TiB_2 phase mainly follows the precipitation-growth process, in which the precipitation and growth of TiB_2 phase proceed quickly at the reaction interface between salts and liquid Al.
3. At a lower temperature [973 K (700 °C)], the precipitation-growth process and dissolution reaction between AlB_2 and Al_3Ti both contribute to the formation of TiB_2. As the reaction time is prolonged, TiB_2 particles with a smaller size can be formed through the process of the dissolution reaction.

REFERENCES

1. A. Mandal, R. Maiti, M. Chakraborty, and B.S. Murty: *Mater. Sci. Eng. A*, 2004, vol. 386, pp. 296–300.
2. Y.F. Han, X.F. Liu, and X.F. Bian: *Compos. A*, 2002, vol. 33, pp. 133–38.
3. M.L. Wang, D. Chen, Z. Chen, Y. Wu, F.F. Wang, N.H. Ma, and H.W. Wang: *Mater. Sci. Eng. A*, 2014, vol. 590, pp. 246–254.
4. G. Han, W.Z. Zhang, G.H. Zhang, Z.J. Feng, and Y.J. Wang: *Mater. Sci. Eng. A*, 2015, vol. 633, pp. 161–68.
5. Z.N. Chen, T.M. Wang, Y.P. Zheng, Y.F. Zhao, H.J. Kang, and L. Gao: *Mater. Sci. Eng. A*, 2014, vol. 605, pp. 301–09.
6. S. Lakshmi, L. Lu, and M. Gupta: *J. Mater. Process. Tech.*, 1998, vol. 73, pp. 160–66.
7. T.X. Fan, G. Yang, and D. Zhang: *Metall. Mater. Trans. A*, 2005, vol. 36, pp. 225–33.
8. C.F. Feng and L. Froyen: *J. Mater. Sci.*, 2000, vol. 35, pp. 837–50.
9. Z.W. Liu, M. Rakita, W. Xu, X.M. Wang, and Q.Y. Han: *Chem. Eng. J.*, 2015, vol. 263, pp. 317–24.
10. Y. Birol: *J. Alloy. Compd.*, 2009, vol. 480, pp. 311–14.
11. G.K. Sigworth: *Metall. Trans. A*, 1984, vol. 15, pp. 277–82.

12. G.P. Jones and J. Pearson: *Metall. Trans. B*, 1976, vol. 7, pp. 223–34.
13. C.D. Mayers, D.G. McCartney, and G.J. Tatlock: *Mater. Sci. Technol. Lond.*, 1993, vol. 9, pp. 97–103.
14. P.S. Mohanty and J.E. Gruzleski: *Acta Metall. Mater.*, 1995, vol. 43, pp. 2001–12.
15. M.M. Guzowski, G.K. Sigworth, and D.A. Sentner: *Metall. Trans. A*, 1987, vol. 18, pp. 603–19.
16. M. Emamy, M. Mahta, and J. Rasizadeh: *Compos. Sci. Technol.*, 2006, vol. 66, pp. 1063–66.
17. H.B. Michael Rajan, S. Ramabalan, I. Dinaharan, and S.J. Vijay: *Mater. Design.*, 2013, vol. 44, pp. 438–45.
18. T.M. Wang, Z.N. Chen, H.W. Fu, J. Xu, Y. Fu, and T.J. Li: *Scrip. Mater.*, 2011, vol. 64, pp. 1121–24.
19. T.M. Wang, H.W. Fu, Z.N. Chen, J. Xu, J. Zhu, F. Cao, and T.J. Li: *J. Alloy. Compd.*, 2012, vol. 511, pp. 45–49.